J. Chem. Sci. Vol. 129, No. 5, May 2017, pp. 601–608. © Indian Academy of Sciences.
DOI 10.1007/s12039-017-1271-9

REGULAR ARTICLE

Studies on dehydrogenation of cyclohexanol to cyclohexanone over mesoporous SiO_2 supported copper catalysts

B SRIDEVI[b], P NAGAIAH[a], A H PADMASRI[c], B DAVID RAJU[a] and K S RAMA RAO[a,*]

[a]Inorganic and Physical Chemistry Division, CSIR-Indian Institute of Chemical Technology, Hyderabad, Telangana 500 007, India
[b]Government Degree College, Gambhiraopet, Karimnagar, Telangana 505 304, India
[c]Government College for Women, Osmania University, Koti, Hyderabad, Telangana 500 095, India
E-mail: ksramarao@iict.res.in

MS received 12 September 2016; revised 22 February 2017; accepted 28 March 2017

Abstract. SBA-15, KIT-6, SiO_2 supported catalysts with 10% Cu loading have been prepared by impregnation techniques. The prepared catalysts have been characterized by BET technique, X-ray diffraction, Temperature programmed reduction (TPR), XPS and N_2O pulse chemisorption techniques. Dehydrogenation of cyclohexanol has been performed over these catalysts in vapour phase at 523 K. SBA-15 and KIT-6 supported copper catalysts showed higher activity than SiO_2 supported Cu catalyst in dehydrogenation of cyclohexanol, which can be attributed to better Cu dispersion, small copper particle size and more number of Cu active species presented on the surface of mesoporous supported catalysts.

Keywords. Cyclohexanol; Cu/SBA-15; Cu/KIT-6; Cu/SiO_2; dehydrogenation.

1. Introduction

Dehydrogenation of propane, ethyl benzene and 2-methyl pyrazine over suitable catalysts are industrially important processes.[1–3] Catalytic dehydrogenation of cyclohexanol to cyclohexanone is an industrially important reaction in the manufacture of nylon because the two major raw materials in producing polyamide fibre are caprolactum and adipic acid, both of which can be obtained from cyclohexanone.[4,5] Copper-based catalysts have been reported for the dehydrogenation of cyclohexanol in liquid or vapour phase.[6,7] A number of investigations have focused on the influence of support, method of preparation, and amount of copper loading on the activity, with the goal of enhancing the conversion of alcohol.[8–13] Copper containing catalysts have been used in the process for dehydrogenation of cyclohexanol to cyclohexanone for many years.[14]

The subject on SBA-15 type mesoporous molecular sieves have been attracted increasing interest by the scientific community particularly in the area of catalysis because of its high surface area, large pore volume and a uniform hexagonal array of cylindrical mesoporous structure. SBA-15 is a purely siliceous mesoporous molecular sieve with uniform hexagonal channels. Zhao *et al.*,[15,16] extended the family of highly ordered mesoporous silicates by synthesizing Santa Barbara Amorphous (SBA), type material with non-ionic block copolymers as structure directing agents in highly acidic media. Application of mesoporous materials in catalysis area becomes popular day by day because of the fact that mesoporous materials can be used as relatively well-described model materials due to their high surface areas, narrow pore size distributions and usually well-defined chemical properties of the surface.[17] Number of reactions, like conversion of synthesis gas, oxidative dehydrogenation of light alkenes or ethyl benzene studied over mesoporous materials continuously grows up.[18–23] Because of its unique features, SBA-15 has been under intensive investigation as a support for a variety of active components.[24–32]

2. Experimental

2.1 *Preparation of SBA-15*

The parent mesoporous SBA-15 silica support was synthesized hydrothermally under acidic medium using triblock co-polymer (P123) as a template and Tetraethyl orthosilicate (TEOS) as silica source according to the previous reports.[33–37] In a typical experiment, 20 g of tri block copoly-

*For correspondence

mer (P_{123}, M/s. Aldrich Chemicals, and USA) was dispersed in a mixture of 560 g of distilled water and 137.5 g of 35% hydrochloric acid (M/s. Loba Chemie, India). Then, 44 g of Tetraethyl ortho silicate (TEOS, M/s. Aldrich Chemicals, and USA) was added under constant stirring conditions at 313 K for 12 h and the mixture was subjected to the hydrothermal treatment at 373 K for 24 h. The resultant slurry was filtered, dried in air at 373 K for 12 h and then calcined in air at 823 K for 8 h at a ramping rate of 1 K min^{-1}.

2.2 *Preparation of KIT-6*

KIT-6 mesoporous silica was synthesized following the procedure available in the literature.[38] In a typical synthesis, a homogeneous solution was obtained by dissolving. 33.3 g of Pluronic P-123 in 1204 g of distilled water with constant stirring at room temperature up to complete dissolution of P-123 in water. 65.8 g of 37 wt% of HCl was added to the solution and stirring was maintained at room temperature overnight. 33.3 g of n-butanol was added to this solution. After 1 h, 71.67 g of TEOS was added to the above mixture and stirring was continued for 24 h at 308 K. The contents were then transferred into an autoclave and heating at 393 K was maintained for 24 h followed by washing with a mixture of water-methanol (1:1). The solid mass was kept in an oven at 373 K overnight. Finally, the white solid product was calcined at 823 K for 8 h in air.

2.3 *Preparation of supported Cu catalysts*

To prepare Cu/SBA-15 catalysts, the parent SBA-15 was dried at 393 K for 6 h prior to impregnation. Requisite amounts of Cu $(NO_3)_2$ dissolved in water were used to impregnate SBA-15. The sample was dried at 393 K for 12 h and calcined at 623 K for 8 h. This catalyst was designated as CS-15. Cu/KIT-6 and Cu/SiO2 were prepared in the same manner and these were designated as CK-6 and CSO, respectively. In all the catalysts, Cu loading was maintained at 10 weight %.

2.4 *Characterization of catalysts*

N_2 adsorption isotherms were recorded on a Tristar 3000 V6.08A instrument (M/s. Micromeritics Instruments Corporation, USA) at 77 K. The samples were out-gassed at 573 K for 4 h before the measurement. BET method was used to calculate the surface areas using the amount of N_2 adsorbed at 77 K. Total pore volume was taken at a relative pressure of 0.99(unit).

X-ray diffraction analysis of the catalysts were carried out on a Ultima-IV (M/s. Rigaku corporation, Japan) X-ray diffractometer using Ni filtered Cu Kα radiation (λ = 1.54 A°) with a scan speed of 4° min^{-1} and a scan range of 2–80° at 40 kV and 20 mA power. The mean crystalline diameters of catalysts were estimated by Scherer equation from the raw data.

The number of active Cu sites followed by Cu-dispersion, metal area and particle size were estimated by N_2O pulse chemisorption technique. For this purpose, a homemade pulse reactor containing an automatic six port valve with a loop of known volume (100 μL) for injecting 6% N_2O-He mixture in number of pulses was fixed at the inlet of quartz reactor. The outlet of the reactor was connected to a thermal conductivity equipped gas chromatograph with Porapak-T column. Briefly 100 mg of catalyst sample was placed at the centre of the reactor between two quart wool plugs and reduced in H_2 flow at 523 K for 3 h followed by replacing H_2 with He carrier gas. The temperature was lowered to room temperature and pulses of 6% N_2O-He mixture was injected until there is no change in the concentration of N_2O. The metallic Cu on the surface of the catalyst is able to react with N_2O in the following equation:

$$2Cu + N_2O \rightarrow Cu_2O + N_2 \quad (1)$$

By using the stoichiometry between Cu N_2O = 2:1, it is possible to find out the number of active Cu atoms present on the surface of the catalysts. The ratio between the number of active Cu atoms and the total number of Cu atoms multiplied by 100 gives the % Cu dispersion. From the concentration of surface Cu atoms (1.47×10^{19} m^{-2}) it is possible to calculate the Cu-metal area. Assuming the Cu particle either in the shape of sphere or cube, it is possible to calculate the Cu-particle size (p) from the following equation:

$$p = (6 \times 10^3)/(\rho \times A_{Cu}) \quad (2)$$

where, 'ρ' is the density of Cu metal and 'A_{Cu}' is the Cu metal area in $m^2\, g_{Cu}^{-1}$. The particle size thus obtained is in nano meters.

Temperature programmed reduction studies tells the presence of reducible species and their interaction either with support or with other constituents of the catalyst. A homemade quartz reactor in which 50 mg of the catalyst sample was placed has been subjected to heating up to 873 K at a heating ramp of 10 K min^{-1} while maintaining 10% H_2–Ar mixure flow (30 cm^3 min^{-1}). The H_2 consumption due to the reduction of metallic oxide was continuously monitored by a thermal conductivity equipped gas chromatograph coupled with standard GC software.

X-ray photoelectron spectroscopy (XPS) analysis of the catalyst was carried out by a Kratos analytical spectrophotometer, with Mg Kα monochromated radiation (1253.6 eV). The residual pressure in the analysis chamber was around 10^{-9} mbar. The binding energy (BE) measurements were corrected for charging effects with reference to the C 1*s* peak of the adventitious carbon (284.6 eV).

2.5 *Activity data*

1 g of the catalyst was placed between two quartz wool plugs at the centre of a fixed bed glass reactor of 14 mm (i.d.) and 300 mm long. Prior to the reaction, the catalyst was reduced in H_2 flow at 553 K for 3 h. For cyclohexanol (CHA) dehydrogenation, the flow rates of CHA and N_2 (carrier gas) were maintained at 1 cm^3h^{-1} and 1200 cm^3h^{-1}, respectively. The temperature of the reaction was fixed at 523 K. The obtained

Table 1. Surface area, pore volume and average pore diameter of catalysts.

Catalyst	S^a_{BET} (m^2g^{-1})	V^b_t (cm^3g^{-1})	D^c (nm)
SBA-15	500	0.95	7.6
KIT-6	711	1.02	5.7
SiO_2	380	0.60	6.3
CS-15	486	0.75	6.2
CK-6	462	0.75	6.5
CSO	270	0.30	4.4

[a]BET surface area
[b]Total pore volume at relative pressure (P/P_0) of 0.95 by single point method
[c]Average pore size

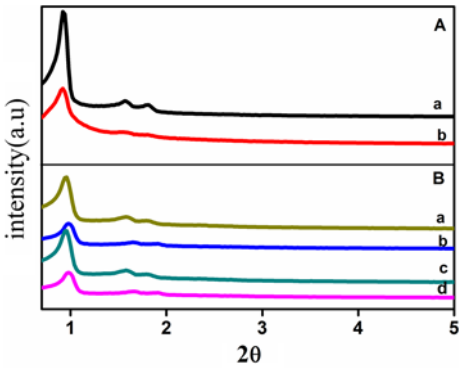

Figure 1. Low angle XRD patterns of (*A*) calcined catalysts (*a*) CS-15, (*b*) CK-6. (*B*) Reduced spent (*a*) CS-15, (*b*) CK-6, (*c*) CS-15, (*d*) CK-6.

products were collected in an ice cooled trap at regular intervals and analyzed by FID-equipped GC-17A (M/s. Shimadzu Instruments, Japan) using ZB WAX capillary column (0.53 mm, i.d, 30 m long) and confirmed by GCMS-QP-5050A (M/s. Shimadzu Instruments, Japan).

3. Results and Discussion

The BET surface area, total pore volume and average pore diameter of the supports and catalysts are shown in Table 1. Compared to SiO_2, SBA-15 and KIT-6 supports possess higher surface area and pore volume. The average pore diameter in these supports is in the range of 5.7 to 7.6 nm. On deposition of Cu over these supports, both surface area and pore volume decrease which are a common phenomena in most of the catalysts. However, there is not much difference in the average pore diameter of copper loaded meso porous materials when compared to that in the supports. In the case of CSO catalyst, the average pore diameter is much lower than that in the SiO_2 support because of the blocking of the pores by Cu particles. The effect of pore blockage by Cu particles is not significant in the case of CS-15 and CK-6 catalysts because of the presence of uniform pores in these supports and most probable smaller Cu particles.

Low angle XRD patterns of calcined catalysts and supports as shown in Figure 1A (XRD patterns of SiO_2 and CSO were not shown as there were no signals in the low angle region) indicate the presence of mesoporosity in these catalysts even after deposition of Cu. The low angle XRD pattern of SBA-15 support exhibited three typical diffraction lines at 0.91–0.97°, 1.60–1.66° and 1.86–1.92°, respectively, on the 2θ scale that are indexed as (100), (110) and (200) reflections associated with *p6mm* hexagonal symmetry. The position of diffraction peaks are well matched with the reported XRD patterns of SBA-15.[12] In the low angle XRD pattern of KIT-6 two well resolved diffraction peaks including four poorly resolved peaks can be observed from Figure 1, which are responsible for ordered mesoporosity of KIT-6. Particularly, the diffraction peaks present at $2\theta = 0.89°$, $2\theta = 1.56^0$ revealing cubic nature of KIT-6 with d_{211}, d_{420} spacing,[39] indicating that these materials possess well-ordered pore arrangement. Low angle XRD patterns of reduced and spent catalysts too witness the presence of mesoporous nature of the supports even after deposition of Cu and after subjecting reduction and cyclohexanol dehydrogenation reaction of the catalysts. The retainment of mesoporosity even after deposition of Cu and after the reaction clearly indicates the robustness of the supports, SBA-15 and KIT-6 with respect to the mesoporous nature.

The wide angle XRD patterns of calcined catalysts are shown in Figure 2A. Presence of Cu^{+2} crystalline phase with d value of 2.52 A^0 at $2\Theta = 35.6^0$, 2.32 at $2\Theta = 38.78^0$ can be seen from this figure (JCPDS NO 5-661). The XRD patterns of reduced and spent catalysts are shown in Figure 2B. Presence of Cu^0 crystalline phase (JCPDS NO.4-836: d value of 2.09 at $2\Theta = 43.25^0$, 1.81 at $2\Theta = 50.37^0$ and 1.28 at $2\Theta = 73.99^0$) can be seen from this picture. Other copper species are not detected in reduced and spent catalysts.

N_2O pulse chemisorption data over supported Cu catalysts has been shown in Table 2. Number of surface Cu atoms is higher in CS-15 followed by CK-6 and in CSO, this number is lowest. Since all the supported Cu catalysts possess same Cu composition (10 weight percent), the Cu dispersion and Cu metal area also follows the same trend as that of number of surface Cu atmos. That is why CSO catalyst contains bigger Cu particles and CS-15 catalyst contains smaller Cu particles. Metal surface coverage and Cu surface density is highest in CS-15 and more or less same in other two catalysts.

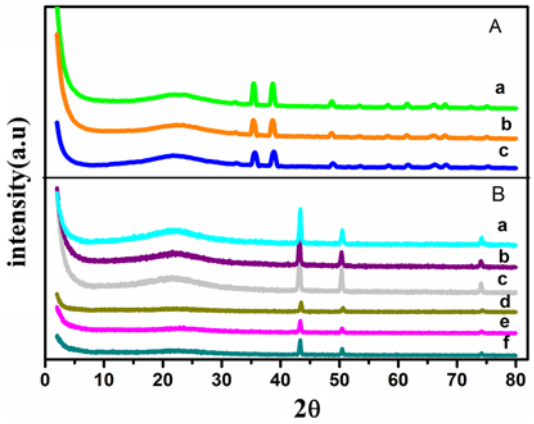

Figure 2. Wide angle XRD patterns of (*A*) Calcined catalysts (*a*) CS-15, (*b*) CK-6, (*c*) CSO. (*B*) Reduced and spent catalysts (*a*) CS-15 Red, (*b*) CK-6 Red, (*c*) CSO Red, (*d*) CS-15 Spent (*e*) CK-6 Spent (*f*) CSO Spent.

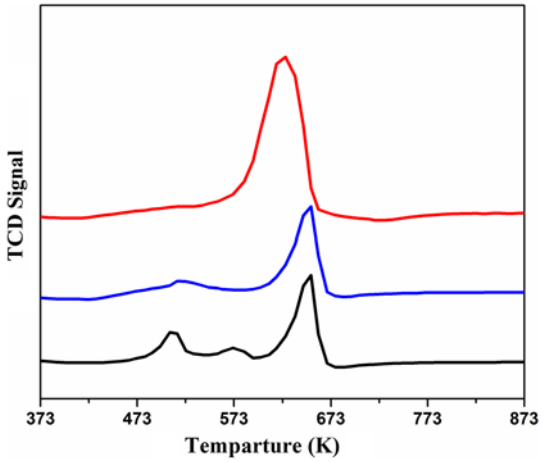

Figure 3. TPR profile of supported copper catalysts (*a*) CS-15; (*b*) CK-6; (*c*) CSO.

This is because of the surface area difference between CK-6 and CSO catalysts.

The extent of reducibility of Cu oxide species in CS-15, CK-6 and CSO catalysts has been measured by H_2-TPR and the TPR profiles are depicted in the Figure 3. TPR patterns of CS-15, CK-6 and CSO witness a high intense reduction signal in the range of 573–673 K may be due to reduction of CuO species interacted with the support. The shifting of Tmax of this signal to higher temperature in CSO and CK-6 indicates the presence bigger Cu species in these catalysts compared to that in CS-6 catalyst. N_2O pulse chemisorption results also support this argument. In CSO and CK-6, CuO gets reduced in two stages; one a small intense signal at low temperature in the range of 473–573 K and other in the temperature ranges of 573–673 K. It is reported that the reduction of dispersed CuO species to Cu^{+1} species takes place in low temperature region (below 573 K), while the bulk CuO gets reduced at high reduction temperatures[40]. The high temperature signal in the temperature range of 573–673 K can be attributed to the reduction of interacted CuO species with the support to Cu^{O} species or due to reduction of Cu^{+1} species to Cu^{0} species on CS-15. Wang *et al.,*[41] have reported three different TPR peaks in the impregnated Cu/SiO_2 catalysts; the major one corresponding to the reduction of larger CuO clusters and the minor ones to the reduction of small CuO clusters and highly dispersed Cu (II) species, respectively. Fridman and Davydov[42] reported the presence of Cu^{0} state in the reduced catalysts. Overall, from the TPR results one can assess that CS-15 catalyst contains large number of uniform sized Cu species resulted from the reduction of a single peak.

The X-ray photoelectron spectroscopy (XPS) is one of the important techniques to explore the oxidation state of transition metal compounds that are having localized valance d-orbitals because of different energies of the photoelectrons. The X-ray photoelectron spectrum of the reduced and spent CS-15 and catalyst is displayed in Figure 4. Here, two distinct peaks corresponding to Cu $2p_{3/2}$ and Cu $2p_{1/2}$ are present at the binding energies of 934 and 954 eV, respectively. The appearance of

Table 2. N_2O pulse chemisorption data of supported Cu catalysts.

Catalyst	BET Surface area ($m^2\ g^{-1}$)	N_2O pulse chemisorptions results				Metal surface coverage area%	Cu surface density
		No. of surface Cu atoms per gram catalyst $\times 10^{-20}$	Cu dispersion (%)	Cu particle size (nm)	Cu Metal surface area ($m^2\ g^{-1}_{catalyst}$)	(Cu Metal area/BET area) $\times$ 100	(No. of Active Cu atoms per unit surface area) $\times 10^{-17}$
CS-15	486	2.06	21.08	4.8	14.0	2.88	4.24
CK-6	462	1.36	14.33	7.2	9.3	2.01	2.95
CSO	270	0.82	8.64	12.0	5.6	2.08	3.04

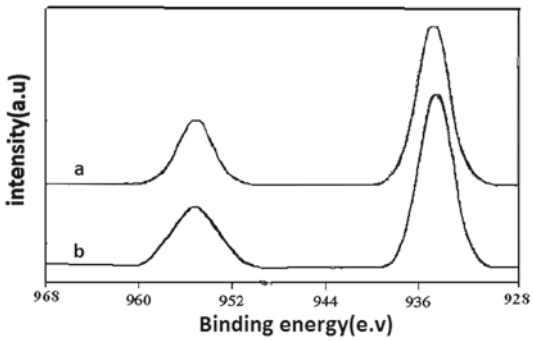

Figure 4. XPS Spectra of (*a*) CS-15 Spent; (*b*) CS-15 reduced catalysts.

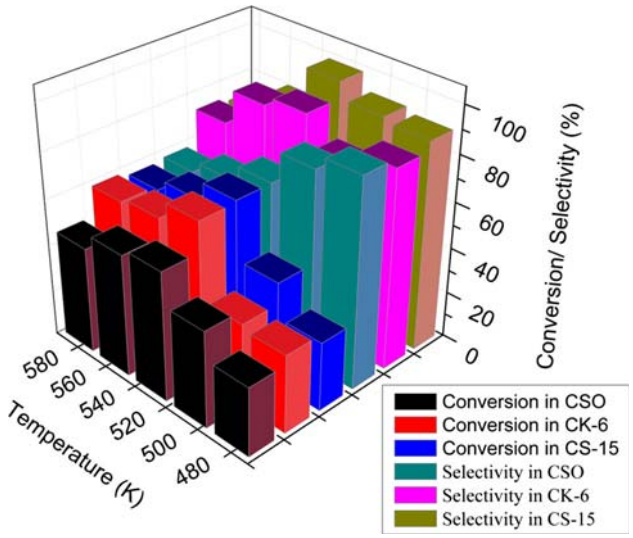

Figure 5. Temperature effect on CSO, CK-6 and CS-15 catalyst.

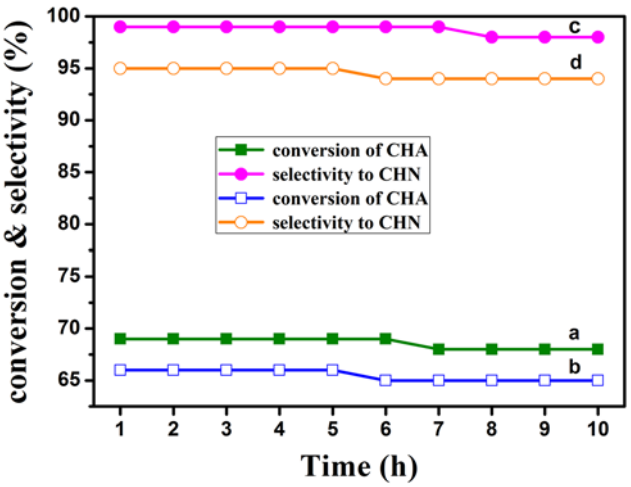

Figure 6. Results of time on stream studies of (*a*) CS-15 and (*b*) CK-6.

the Cu $2p_{3/2}$ main peak at the binding energy of 934 eV demonstrates the presence of Cu^0 in the CS-15 catalyst. In fact, transition metal ions are well-reported[43,44] to have unfilled 3d orbital that show well-separated satellite peaks in the core level XP spectra due to electron shake-up and the structure of satellite; i.e., the peak number, intensity and splitting, reflect the nature of chemical bonding of the transition metal ions. In the case of Cu based catalysts, these satellites have been attributed to the shakeup transitions by ligand → metal 3d charge transfer which is very characteristic of Cu^{2+} compounds and is not seen in Cu^+ compounds or in metallic Cu because of completely filled 3d shells.[45] In the present case, the absence of these satellite peaks clearly indicates the absence of Cu^{2+} species.

Figure 5 consolidates the activity results at different temperatures in the range of 473–573 K over CSO, CK-6 and CS-15 catalysts. On all the catalysts, conversion of cyclohexanol follows an increasing trend with temperature. However, cyclohexanol conversion is higher on CK-6 and CS-15 catalysts. The selectivity over CSO catalyst gradually decreases with temperature, whereas it increases with temperature up to 548 K and thereafter decreases over CK-6 and CS-15 catalysts. Cyclohexanol dehydrogenation is an endothermic reaction and therefore increases in the cyclohexanol conversion and selectivity to cyclohexanone and thereby in the yield of cyclohexanone is not a surprising phenomenon. Cyclohexanol reaction is an equilibrium controlled reaction and therefore it is difficult to achieve 100% conversion without the presence of oxidants at 473 and 513 K.[46,47] Higher cyclohexanol conversion and cyclohexanone selectivity possessed by CK-6 and CS-15 is due to their higher surface area and uniform pore size which are helpful in dispersing Cu sites uniformly. 2D hexagonal structure of SBA-15 and 3D cubic structure of KIT-6 with mesoporous character as evidenced by low angel XRD and more surface area leads to better copper dispersion, smaller particle size which influences the activity. Larger BET surface area inhibits the sintering of copper particles to some extent.[48,49] Sivaraj *et al.*, have reported a similar result between the conversion and the copper surface area for the same reaction over Cu/alumina catalyst.[50,51] Thus KIT-6 and SBA-15 with larger surface area can be regarded as better supports for Cu catalysts than SiO_2. CK-6 and CS-15, therefore are subjected for time on stream study.

Figure 6 shows the steady cyclohexanol conversion and cyclohexanone selectivity over CS-15 and CK-6 catalysts during 10 h in an on-stream study. Between these two catalysts, CS-15 seems to be a better catalyst in terms of maintaining both cyclohexanol conversion and cyclohexanone selectivity. Higher Cu dispersion with smaller Cu particle size in CS-15 is the reason for its

Table 3. Comparison of activity of present catalyst with those reported in the literature.

Catalyst	Wt% Copper	Cyclohexanol Conversion %	Cyclohexanone Selectivity %	Reference
Cu-MgO	24	59	89	14
Cu-Mgo-Cr_2O_3	22	65	97	14
Commercial Cu-Cr_2O_3	24	35	70	14
Cu-ZnO-Al_2O_3	20	52	85	51
Cu-ZnO	25	56	98	6
CuO-ZnO-Cr_2O_3	45	62	97	39
Cu-SBA-15	10	70	99	Present work
Cu-KIT-6	10	69	92	Present work

better performance. Table 3 clearly indicates that the performance of present catalyst is either on par or better than the reported catalysts.

Popova *et al.,* have compared the cyclohexanol dehydrogenation capability of Cu /Al_2O_3 and Cu/SiO_2 catalysts and found that Cu/SiO_2 exhibits more selective formation of cyclohexanone than on Cu/Al_2O_3 because of its low acidity.[52] On the other hand, the present study is aimed to show the advantages of Cu/SBA-15 and Cu/KIT-6 catalysts in terms of uniform mesoporosity which is helpful in yielding higher cyclohexanol dehydrogenation ability than on Cu/SiO_2 catalyst (Figure 5). The mesoporous nature of SBA-15 and KIT-6 is able to disperse Cu particles nicely than in Cu/SiO_2 (Table 2).

4. Conclusions

Better dispersion of Cu over mesoporous SiO_2 structures like SBA-15 and KIT-6 is the main reason for the excellent performance of CS-15 and CK-6 catalysts.

Supplementary Information (SI)

Crystallographic data (excluding structure factors) for the structure in this paper have been deposited with the Cambridge Crystallographic Data Centre, CCDC, 12 Union Road, Cambridge CB21EZ, UK. Copies of the data can be obtained free of charge on quoting the depository numbers CCDC number: 784651 or 1 (Fax: +44-1223-336-033; E-mail: deposit@ccdc.cam.ac.uk, http://www.cam.ac.uk)

Acknowledgements

BS and PN thank CSIR and UGC, New Delhi, India for the award of Junior Research Fellowship.

References

1. Koc S N, Dayioglu K and Ozdemir H 2016 Oxidative dehydrogenation of propane with K-MoO_3/$MgAl2O_4$ catalysts *J. Chem. Sci.* **128** 67
2. Pochamoni R, Narani A, Varkolu M, Muralidhar G, Sai Prasad P S, David Raju B and Rama Rao K S 2015 Studies on dehydrogenation with CO_2 as soft oxidant over Co_3O_4/COK-12 catalysts *J. Chem. Sci.* **127** 701
3. Jing F, Zhang Y, Luo S, Chu W, Zhang H and Shi X 2010 Catalytic synthesis of 2-methylpyrazine over Cr-promoted copper based catalyst via a cyclo-dehydrogenation reaction route *J. Chem. Sci.* **122** 621
4. Chen W S and Lee M D 1992 Nonoxidative dehydrogenation of cyclohexanol over copper-iron binary oxides *Appl. Catal.* **83** 201
5. Jeon G S and Chung J S 1994 Preparation and characterization of silica-supported copper catalysts for the dehydrogenation of cyclohexanol to cyclohexanone *Appl. Catal.* **29** 115
6. Krishna G, Rama Rao K S and Kanta Rao P 1999 Effect of support modification by carbon coverage in the dehydrogenation activity of Cu/Al_2O_3 Catalyst *Catal. Lett.* **59** 157
7. Mendes F M T and Schmal M 1997 The cyclohexanol dehydrogenation on Rh-$CuAl_2O_3$ catalysts PART 1: Characterization of catalysts *Appl. Catal. A* **151** 393
8. Nikiforova N N and Gavrenko K A 1974 4th EFCATS School on Catalysis catalyst design – from molecular to industrial level *Petrochemisry (in Russian)* **14** 11
9. Sing K S W, Everett D H, Haul R A W, Moscou L, Pierotti R A, Rouquerol J and Siemieniewska T 1985 Hybrid inorganic–organic mesoporous silicates—nanoscopic reactors coming of age *Pure Appl. Chem.* **57** 603
10. Chang H F and Saleque M A 1993 Surface Structure and Catalytic Properties of Cu/SiO_2 Catalysts Prepared by Different Methods *Appl. Catal. A* **103** 233
11. Burri D R, Jun K W, Kim Y H, Kim J M, Park S E and Yoo J S 2002 Oxidative Cleavage of C=C Bond of Styrene and Its Derivatives with H_2O_2 using Vanadyl (IV) Acetylacetonate Anchored SBA-15 Catalyst *Chem. Lett.* **31** 212
12. Huizhen L, Jiang T, Han B, Liang S and Zhou Y 2009 Selective phenol hydrogenation to cyclohexanone over a Dual Supported Pd-Lewis Acid Catalyst *Science* **326** 1250
13. Chag H F, Salequ M A, Hsu W S and Lin W H 1996 Characterization and dehydrogenation activity of $CuAl_2O_3$ catalysts prepared by electroless plating technique *J. Mol. Catal.* **109** 249

14. Nagaraja B M, Siva Kumar V, Shashikala V, Padmasri A H, Sreevardhan Reddy B, Reddy S, David Raju B and Rama Rao K S 2004 Effect of method of preparation of copper–magnesium oxide catalyst on the dehydrogenation of cyclohexanol *J. Mol. Catal. A* **223** 339
15. Reddy S S, Burri D R, Kumar S V, Padmasri A H, Narayanan S and Rama Rao K S 2007 Sulfonic acid functionalized mesoporous SBA-15 for selective synthesis of 4-phenyl-1, 3-dioxane *Catal. Commun.* **8** 261
16. Zhao D, Feng J, Huo Q, Melossh N, Fredrickson G H, Chmelka B F and Stucky G D 1998 Triblock copolymer syntheses of mesoporous silica with periodic 50 to 300 angstrom pores *Science* **279** 548
17. Zhao D, Huo Q, Feng J, Chmelka B F and Stucky G D 1998 Mesocellular Siliceous Foams with Uniformly Sized Cells and Windows *J. Am. Chem. Soc.* **120** 6024
18. Wang H, Li L, Bai X F, Shang J Y, Yang K F and Xu L W 2013 Efficient Palladium-Catalyzed C-O Hydrogenolysis of Benzylic Alcohols and Aromatic Ketones with Polymethylhydrosiloxane *Adv. Synth. Catal.* **355** 341
19. Takahashi T, Yoshimura M, Suzuka H, Maegawa T, Sawama Y and Monguci Sajiki H 2012 Chemoselective hydrogenation using molecular sieves-supported Pd catalysts: Pd/MS3A and Pd/MS5A *Tetrahedron* **68** 8293
20. Rodiansono, Khairi S, Hara T, Ichikuni N and Shimazu S 2012 Highly efficient and selective hydrogenation of unsaturated carbonyl compounds using Ni–Sn alloy catalysts *Catal. Sci. Technol.* **2** 2139
21. Mirkhani V, Moghadam M, Tangestaninejad S, Mohammadpoor-Baltork I and Rasouli N 2008 A comparative study of oxidation of alkanes and alkenes by hydrogen peroxide catalyzed by Cu(salen) complex covalently bound to a Keggin type polyoxometalate and its neat counterpart *Catal. Commun.* **9** 2411
22. Anand N, Reddy H P K, Swapna V, Rama Rao K S and Burri D R 2011 Fe(III) complex anchored SBA-15 is a new heterogeneous catalyst for the cleavage of aliphatic C-C bond of styrene and its derivatives *Micropor. Mesopor. Mater.* **143** 132
23. Qiu T, Xua X and Qian X 2009 Fluorous biphase oxidation of ethyl benzene and benzyl alcohol catalyzed by perfluoroalkyl phthalocyanine complexes *J. Chem. Technol. Biotechnol.* **84** 1051
24. Tanase S, Reedijk J, Hage R and Rothenberg G 2010 Hydrocarbon oxidation with H_2O_2, catalyzed by iron complexes with a polydentate pyridine-based ligand *Top. Catal.* **53** 1039
25. Mishra G S, Anil Kumar and Tavaresa P B 2012 Single site anchored novel Cu (II) catalysts for selective liquid–gas phase O_2 oxidation of n-alkanes *J. Mol. Catal. A: Chem.* **357** 125
26. Rioux R M, Song H, Hoefelmeyer J D, Yang P and Somorjai G A 2005 High surface area catalyst design: synthesis, characterization, and reaction studies of platinum nanoparticles in mesoporous SBA-15 silica *J. Phys. Chem.* **109** 2192
27. Sun J, Ma D, Zhang H, Liu X, Han X, Bao X, Weinberg G, Pfander N and Su D 2006 Toward monodispersed silver nanoparticles with unusual thermal stability *J. Am. Chem Soc.* **128** 15756
28. Lopes I, Hassan N E, Guerba H, Wallez G and Davidson A 2006 Size-induced structural modifications affecting Co_3O_4 nanoparticles patterned in SBA-15 silicas *Chem. Mater.* **18** 5826
29. Segura Y, Cool P, Kustrowski P, Chmielarz L, Dziembaj R and Vansant E F 2005 Characterization of vanadium and titanium oxide supported SBA-15 *J. Phys. Chem. B* **109** 12071
30. Yang C M, Liu P H, Ho Y F, Chiu C Y and Chao K J 2003 Highly dispersed metal nanoparticles in functionalized SBA-15 *Chem. Mater.* **15** 275
31. Feng X, Yan M, Zhang T, Liu Y and Bao M 2010 Preparation and application of SBA-15-supported palladium catalyst for Suzuki reaction in supercritical carbon dioxide *Green Chem.*12 1758
32. Zhao M, Church T L and Harris A T 2011 SBA-15 supported Ni-Co bimetallic catalysts for enhanced hydrogen production during cellulose decomposition *Appl. Catal. B* **101** 522
33. Wang H and Liu C J 2011 Preparation and characterization of SBA-15 supported Pd catalyst for CO oxidation *Appl. Catal. B* **106** 672
34. Palcheva R, Spojakina A, Dimitrov L and Jiratovac K 2009 12-Tungstophosphoric heteropolyacid supported on modified SBA-15 as catalyst in HDS of thiophene *Micropor. Mesopor. Mater.* **122** 128
35. Zukal A, Pastva J and Cejka J 2013 MgO-Modified Mesoporus Silicas impregnated by potassium *Micropor. Mesopor. Mater.* **167** 44
36. Burri D R, Choi K M, Lee J H, Han D S and Bark S E 2007 Influence of SBA-15 support on $CeO_2 - ZrO_2$ catalyst for the dehydrogenation of ethylbenzene to styrene with CO_2 *Catal. Commun.* **8** 43
37. Burri D R, Shaikh I R, Choi K M and Park S E 2007 Facile heterogenization of homogeneous ferrocene catalyst on SBA-15 and its hydroxylation activity *Catal. Commun.* **8** 731
38. Kleitz F, Choi S H and Ryoo R 2003 Cubic Ia3d large mesoporous silica: Synthesis and replication to platinum nanowires, carbon nanorods and carbon nanotubes *Chem. Commun*. **17** 2136
39. Kim T W, Kleitz F, Paul B and Ryoo R 2005 MCM-48-like large mesoporous silicas with tailored pore structure: Facile synthesis domain in a ternary triblock copolymer-butanol- water system *J. Am. Chem. Soc*. **127** 7601
40. Venkateswarlu V, Saidulu G, Ravikumar M, Rama Rao K S and David Raju B 2014 Vapor phase chemoselective conjugate hydrogenation of isophorone over Pd/SBA-15 catalysts *Ind. J. Chem.* **53A** 557
41. Wang Z, Liu Q, Yu J, Wu T and Wang G 2003 Surface structure and catalytic behavior of silica-supported copper catalysts prepared by impregnation and sol–gel methods *Appl. Catal. A: Gen.* **239** 187
42. Fridman V Z and Davydov A A 2000 Dehydrogenation of cyclohexanol on copper-containing catalysts: I. The influence of the oxidation state of copper on the activity of copper sites *J. Catal.* **195** 20
43. Rioux R M and Vannice M A 2003 Hydrogenation/dehydrogenation reactions: Isopropanol dehydrogenation over copper catalysts *J. Catal.* **216** 362
44. Chang F W, Yang H C, Roselin L S and Lee W Y 2006 Ethanol Dehydrogenation Over copper Catalysts on Rice husk ash prepared by ion exchange *Appl. Catal.* **304** 30

45. Frost D C, Ishitani A and McDowell C A 1972 X-ray photoelectron spectroscopy of copper compounds *Mol. Phys.* **24** 861
46. Carlson T A 1975 In *Photoelectron and Auger Spectroscopy* (New York: Plenum Press)
47. Kim K S 1974 Charge transfer transition accompanying X-ray photoionization in transition-metal compounds *J. Electron Spectrosc. Relat. Phenom.* **3** 217
48. Lin Y M, Wang I and Yeh C T 1988 Activity stability of a copper (II) oxide—zinc (II) oxide catalyst for oxidative dehydrogenation of cyclohexanol to cyclohexanone *Appl. Catal.* **41** 53
49. Martin J M C, Guerrero-Ruiz A and Fierro J L G 1995 Structural and surface properties of CuO-ZnO-Cr_2O_3 catalysts and their relationship with selectivity to higher alcohol synthesis *J. Catal.* **156** 208
50. Sivaraj C, Srinvas S T, Rao V N and Rao P K 1990 Selectivity dependence on the acidity of copper-alumina catalysts in the dehydrogenation of cyclohexanol *J. Mol. Catal.* **60** L23
51. Sivaraj C, Reddy B M and Rao P K 1988 Selective dehydrogenation of cyclohexanol to cyclohexanone on Cu-ZnO-Al_2O_3 catalysts *Appl. Catal.* **45** Lll
52. Popova M, Domitrov M, Dal Santo V, Ravasio N and Scotti N 2012 Dehydrogenation of cyclohexanol on copper containing catalysts: The role of the support and the preparation method *Catal. Commun.* **17** 150